ISSN 0005–1144
ATKAAF 42(1–2), 45–51 (2001)

Viktor Valouch, Jiří Škramlík, Ivo Doležel

High-Frequency Interferences Produced in Systems Consisting of PWM Inverter, Long Cable and Induction Motor

UDK 621.313.333
IFAC IA 5.5.4;4.7.1

Preliminary communication

The operation of inverter-fed asynchronous motor drives is inherently accompanied by high-frequency interferences caused particularly by parasitic currents of the common and differential modes. These emissions propagated by conduction and radiation may unfavourably affect the operation of nearby telecommunication and signal cables and various low-current devices. The paper deals with an analysis of these phenomena based on theoretical considerations and results of special measurements of the common and differential mode disturbances. Evaluated are mainly the frequency characteristics of selected parts of the system and their contributions to the resultant harmonic spectra.

Key words: common mode currents, differential mode currents, high-frequency interferences, induction motor, parasitic phenomena

1. INTRODUCTION

Application of advanced semiconductor elements in the modern voltage inverters allows substantial raise of their switching frequency. Consequently, the delivered trapezoidal voltage pulses reach considerably high values of du/dt (often more than 10 kV/μs). Situation in a system consisting of the PWM inverter, feeding cable and induction motor (IM) is then strongly influenced by its leakage capacitances and characterised by circulation of the high-frequency parasitic common and differential mode currents. These currents may produce, beside various overvoltages and growth of additional losses in the motor and inverter, electromagnetic interferences (EMI) propagated into the surroundings as conducted and radiated emissions. These interference signals are (by the corresponding standards) divided into two groups: those produced by harmonics up to 9 kHz and those generated by very fast changes of voltage in the semiconductor devices (in the intervals 9–150 kHz and 150 kHz–30 MHz, respectively).

The electromagnetic interferences can unfavourably affect operation of the telecommunication or signal cables parallel with the supplying power cable and also other near low-current devices.

Analysis of the indicated phenomena is extremely difficult and requires correct mathematical models of all parts of the system. This includes good distributed-parameter representations of both induction motor and feeding cable and a sufficiently sophisticated model of the inverter. At present, several separate high-quality models exist that enable modelling some elements of the system (cable, IM) [1]. On the other hand, the influence of the inverter itself and behaviour of the whole system have not systematically been studied yet. That is why the problems associated with the interferences and related effects are explored mainly experimentally and the calculation procedures are prevailingly formula-ted within the frequency domain.

The paper indicates the starting points and methodology of evaluation of the interferences, discusses advantages and drawbacks of various models and shows some important results obtained by means of measurements (common and differential mode disturbances and frequency characteristics of individual parts of the system).

2. COMMON AND DIFFERENTIAL MODE MECHANISMS

In PWM voltage source inverters the common and differential mode currents occur simultaneously in their standard mode of operation. Their paths are depicted in Figure 1.

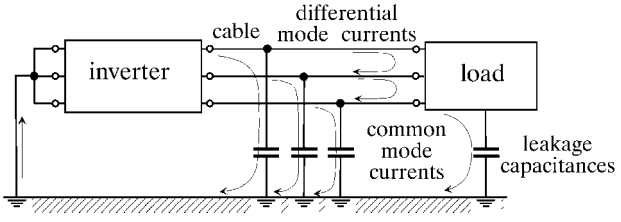

Fig. 1 Circulation of the common and differential mode currents in the system

The common mode currents are generated by the output voltage pulses of the inverter. The waveforms of the pulses are trapezoidal, with very high values of du/dt following from the switch-on and switch-off times of the power semiconductor elements. The changes of voltages on different parasitic capacitances (for instance capacitances between the semiconductor chips and ground or between the motor case and ground) produce the common mode currents passing through earth, the power mains and/or other elements back to their source, see Figure 2.

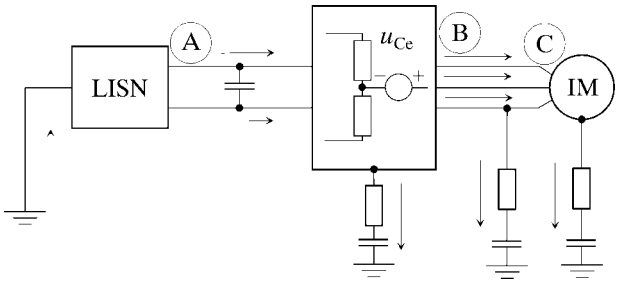

Fig. 2 Paths of the common mode currents in an IM drive

The figure contains a simplified equivalent diagram of one phase of the inverter for the common mode. If the LISN (Line Impedance Stabilisation Network that isolates the stage of the drive from the mains) is used as a fixed artificial network and measurement point, these currents are observed at the LISN as the common mode noise.

The differential mode currents are excited by semiconductor current pulses that are characterised by steep peaks of reverse recovery currents of freewheeling diodes. These currents flow via phases of the IM and/or through the D.C. link of the inverter generating the differential mode noise at the LISN, see Figure 3.

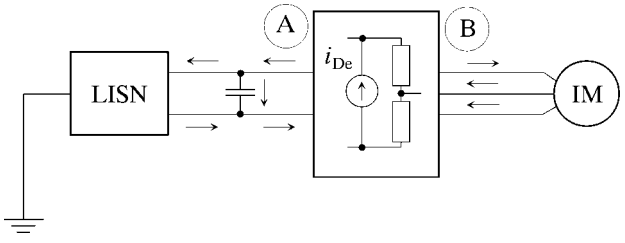

Fig. 3 Paths of the differential mode currents in an IM drive

Figure 4 shows an exciting trapezoidal voltage pulse of the inverter with its spectrum envelope.

In order to generate the common mode currents, a specific control strategy has to be used. The strategy is that all three inverter output terminals are connected simultaneously to either plus or minus busbar of the D.C. link. The voltage changes of U_d occur on the parasitic capacitance between the IM case and ground, producing the common mode interferences.

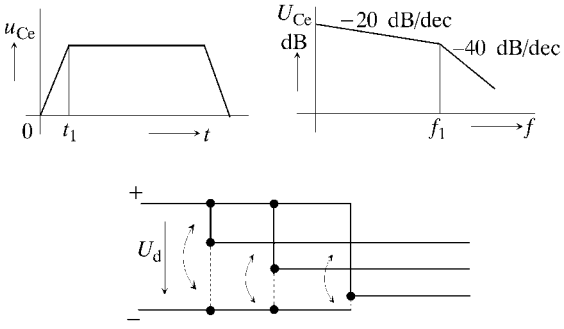

Fig. 4 Exciting voltage signal in the common mode and its generation

Figure 5 shows the waveform of the current pulse flowing through the switching element of the inverter during the switch-on process. A control strategy of the inverter, producing just only the differential mode interferences, is depicted in the figure, too.

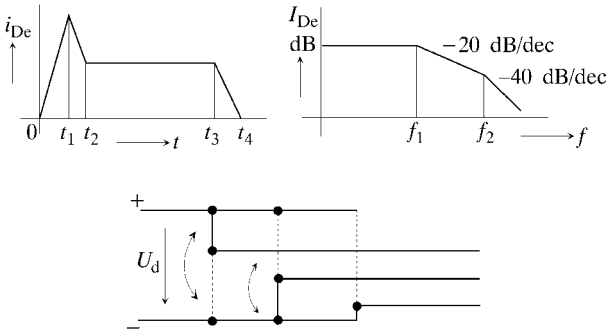

Fig. 5 Exciting current signal in the differential mode and its generation

Both described strategies can be used for excitation of the common and differential modes separately. The IM remains in the standstill during the measurements. In most PWM strategies for A.C. motor drives, however, both the modes are produced simultaneously within the fundamental period. Thus, a special measuring circuits or techniques have to be used for separation of these modes.

3. THEORETICAL BACKGROUND

A high-frequency lumped-parameter model of the IM was presented in [2]. The model consisted of two parts similar in their structures but generally different in parameter values. Starting from that model, the equivalent circuits for both modes (for

frequency range up to about 1 MHz) were suggested, in common with their transfer functions. This IM model can be generalised by assuming n similar blocks connected in series; such a model may better simulate operation of the IM within a substantially wider range of frequencies. Nevertheless, it is first necessary to overcome the principal problem: how to determine appropriate values of the parameters of the model for n being higher than 3. This represents a complicated problem even with knowledge of the measured IM data and sophisticated SW optimisation tools.

Also the feeding cables may be analysed more precisely than in [2] using models with distributed parameters and respecting their dependence on frequency. However, complexity of models of the system comprising the cable and IM becomes substantially higher.

The inverter may be represented in the respective frequency range either by its circuit model [3] or by a transfer function in the frequency domain [4]. An appropriate circuit model must include elements representing all relevant parasitic links manifesting themselves in the high frequency range. With respect to difficulties associated with determining the values of the circuit elements, the second approach seems to be more convenient. Figure 6 shows the transfer characteristics between points A and B (see Figure 2) for the common mode, measured at the Mitsubishi IGBT voltage-source inverter. The figure shows the amplitude of the output signal for injected AC input signal with the amplitude of 100 mV. Thus, the curve may be viewed as a frequency transfer characteristic with the amplitude lower than 1. The transfer function may be used for the prediction of the interference spectra produced by different parts of the drive, provided that the excitation voltage (in the common mode) or current signal (in the differential mode) is known.

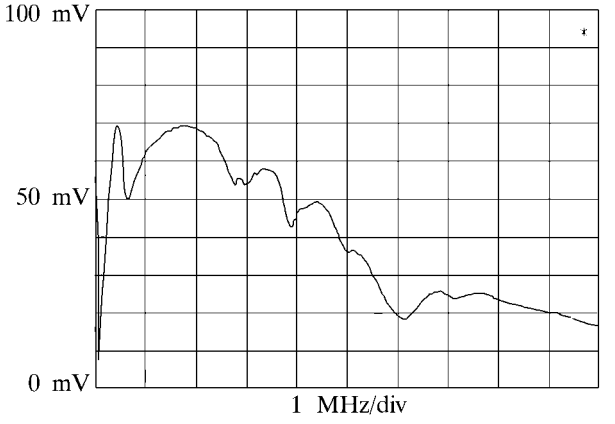

Fig. 6 Transfer characteristic between points A and B (see Figure 2), common mode

In order to analyse the whole drive in the frequency domain, all its principal parts (inverter, cable, IM) have to be represented there together with their mutual interactions. So the frequency characteristics themselves of the cable and IM in a wide frequency range and ideas about influence of the principal parts of the drive on the total frequency spectrum seem to be expedient.

The interference fields themselves are generally 3D and non-stationary. Their distribution is mostly described by non-linear second-order partial differential equations of the (in dependence on the frequency of the field quantities) elliptical, parabolic or hyperbolic types. Exact solutions to these equations in larger areas are, unfortunately, unavailable so far, even with the most sophisticated SW tools. The present methods for solution of such tasks are based, therefore, on certain simplifying assumptions:

- any back influences of the disturbed parts are neglected,
- the sources of EMI as well as all surrounding media have linear properties (their values are independent of the frequency and field quantities),
- solved are only the steady states; for example, the inverter is supposed to deliver a series of voltage pulses having the character of a perfectly periodical function.

In case of the investigated system the solution starts from the determination of the field producing quantities (the common and differential mode currents). The series of voltage pulses is first decomposed into individual harmonics for which the corresponding common and differential current responses have to be found. Correctness of the results depends on the quality (structures and parameters) of the mentioned equivalent circuits and their transfer functions or field models of the main parts of the system. Further problems may occur, for example, with incorporation of the shielding, grounding etc. Superposition of the respective responses then yields the resultant currents and character of the disturbances, mostly in the frequency domain.

The following step is to find the time dependencies of the common and differential mode currents. This is, particularly in case of the distributed parameter representation of the system, often possible only by means of suitable numerical methods (FDM or special procedures for the back Laplace transform), whose use may be accompanied by uneasily estimable errors. At this moment, however, all necessary data for the consequent calculation of the interference field distribution are known.

The high frequency field computation starts from the Maxwell equations

$$\text{rot}\left(\frac{1}{\mu}\boldsymbol{B}\right) = \boldsymbol{J} + \varepsilon\frac{\partial \boldsymbol{E}}{\partial t}, \qquad \text{rot}\,\boldsymbol{E} = -\frac{\partial \boldsymbol{B}}{\partial t}. \tag{1}$$

As mentioned before, these equations are generally non-linear and time-dependent. Let's have a look at one of the common arrangements depicted in Figure 7.

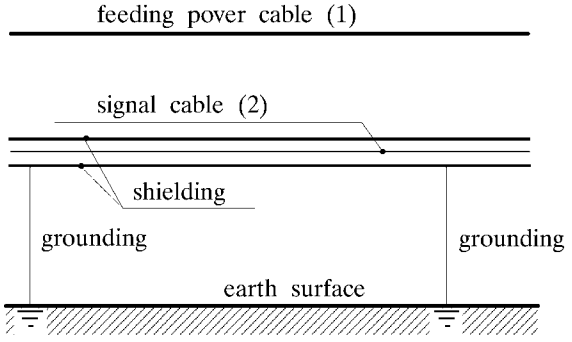

Fig. 7 Parallelism of cables with shielding elements

Because of the eddy currents induced in the shielding sheaths or grounded metal constructions the field has to be described by magnetic vector potential $\boldsymbol{A}$. Due to high frequencies the displacement currents should also be respected in the first Maxwell equation. The equation describing the vector potential distribution (derived from system (1)) produced by respective current harmonics then reads

$$\nabla \times \frac{1}{\mu}\nabla \times \boldsymbol{A} + j\omega\gamma\boldsymbol{A} - \varepsilon\omega^2\boldsymbol{A} = \boldsymbol{J}, \tag{2}$$

where ε, γ and μ denote the permittivity, electrical conductivity and permeability of the medium, respectively, and $\boldsymbol{J}$ denotes the amplitude of the field current density of the given harmonic in the power cable. Uniqueness of solution of (1) is assured by imposing the correct boundary conditions.

Unfortunately, the described electromagnetic field generally shows 3D features and must be determined for a wide spectrum of important harmonics. This is possible only by means of highly specialised and expensive SW based on purely numerical methods. Further problems follow from the presence of incommensurable subregions in the investigated domain (small volumes of the conductors and metal parts and by several orders larger volumes of surrounding media such as air or earth). That is why a simplified way of computation is often used consisting in solution of a series of 2D fields in selected sufficiently large planes perpendicular to the direction of the cables. Discretisation of these planes is much easier and due to constant parameters of all media the calculations run at a substantially higher rate. The field distribution between any two neighbour planes may be determined by suitable interpolation.

4. EXPERIMENTAL SET-UP

The basic arrangement for measurements of the conducted emissions is in Figure 8.

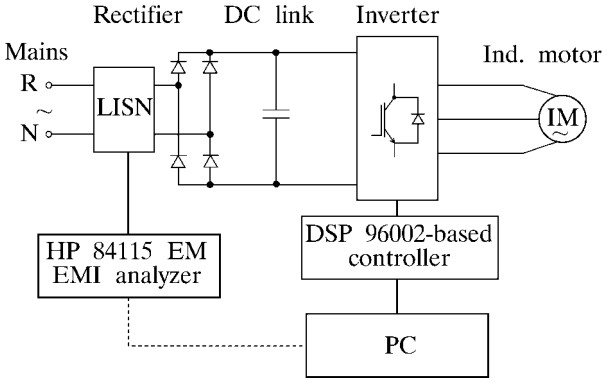

Fig. 8 Basic arrangement for measurement of the conducted emissions

An induction motor 1.5 kW was connected to the Mitsubishi IGBT inverter through a cable (of varying lengths). The inverter was fed from a bridge rectifier via a D.C. link. The DSP-96002-based controller provides a possibility to control each of the inverter elements independently in accordance with the strategy selected. The inverter can work not only with the PWM strategy, but also generate either only common or only differential mode disturbances. For measurements of the frequency characteristics of different parts of the drive the scheme was suitably modified. The 4284 A precision RLC meter and Le Croy 9354 AM oscilloscope were used for the measurement of impedances and time responses, respectively.

5. MEASUREMENTS OF CONDUCTED EMISSIONS

Figures 9, 10 and 11 show the common mode interference spectra detected at the measurement point in the LISN and expressed in the double logarithmic representation for three different lengths of the feeding cables ($l_c = 2$, 10 and 30 m). Three characteristics are depicted in each figure, namely for only the inverter in operation (dotted lines), the inverter with the feeding cable (dashed lines) and for the inverter feeding the IM through the cable (full lines).

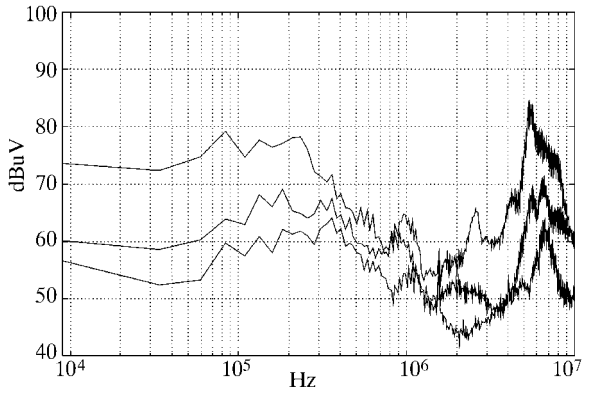

Fig. 9 Common mode interference spectra ($l_c = 2$ m)

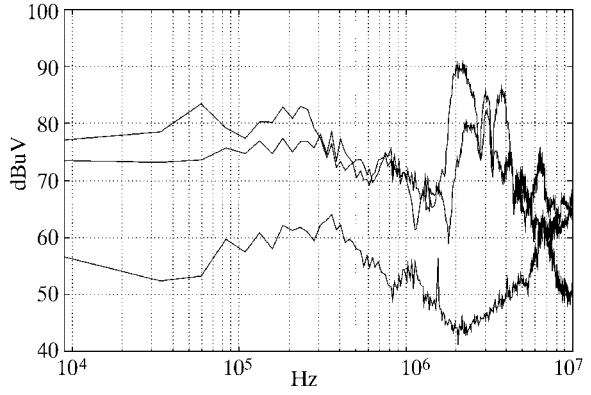

Fig. 10 Common mode interference spectra ($l_c = 10$ m)

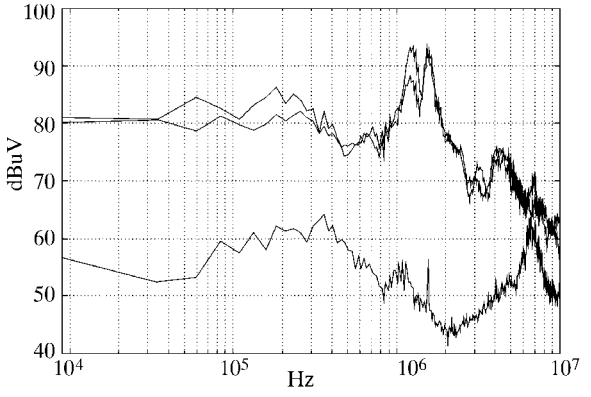

Fig. 11 Common mode interference spectra ($l_c = 30$ m)

Two main peaks (around 350 kHz and 6.5 MHz) may be recognised at the frequency spectrum for the inverter working alone without any load. After comparing the curves in all three figures we can see that the longer is the cable, the higher is the level of the common mode interference (dashed lines), while for the longest cable the spectra measured without and with the induction machine (Figure 11) are almost identical.

With growing lengths of the cable the current flowing via the stray capacitances of the cable to ground increases, too. For a certain length of the cable the contribution of the IM leakage current to the total current is almost negligible, except for the range of lower frequencies (below a few hundreds of kHz). It is clearly visible that the character of the spectra (full lines) between 70 and 300 kHz is practically the same irrespective of the lengths of cables feeding the IM. On the contrary, the second dominating part of the characteristics (around 5.5, 2.5 and 1.5 MHz in Figures 9, 10 and 11) depends on the cable length (2, 10 and 20 m, respectively).

Figure 12 compares the time responses of the voltages for the cable of length of 2 m (Figure 12a) and 10 m (Figure 12b). In addition to the voltage at

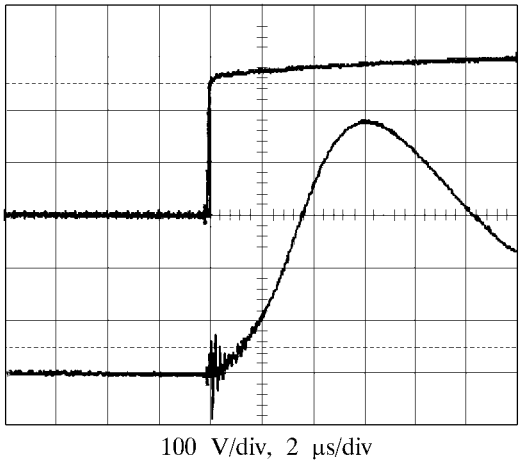

Fig. 12a Time responses of the voltages at the output of the inverter and at the neutral point of the IM ($l_c = 2$ m)

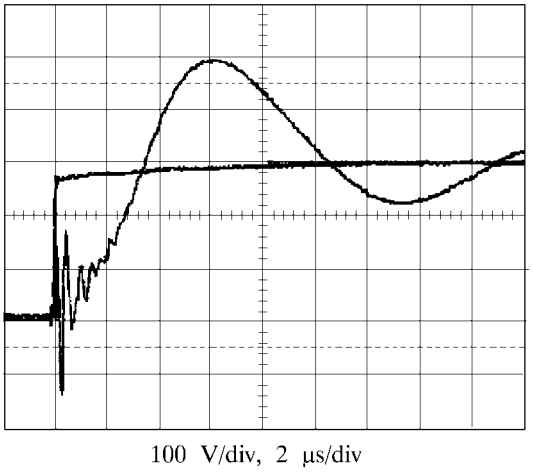

Fig. 12b The time responses of the voltages at the output of the inverter and at the neutral point of the IM ($l_c = 10$ m)

the output of the inverter, the voltage at the neutral point of the IM stator winding is also shown. While the lower frequency of about 70 kHz of transients does not depend on the cable length, the higher frequency changes in dependence on the cable length and in accordance with the spectra shown in Figures 9 and 10 (5.5 and 2.5 MHz).

Figure 13 presents the low frequency part of the amplitude characteristic for the inverter feeding the IM (see Figure 10) expressed by using the linear vertical scale. The shape of this part of the characteristic well indicates the contribution of the IM to the total common mode interference.

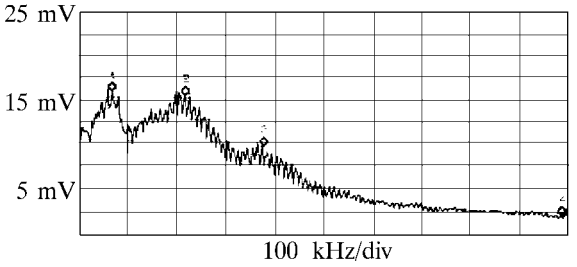

Fig. 13 The low frequency part of the amplitude characteristic of the

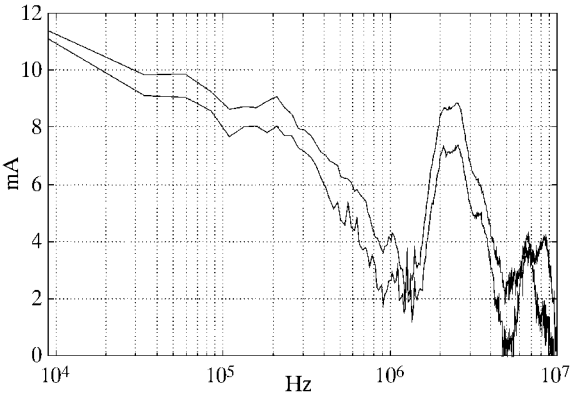

Fig. 14 Amplitude frequency spectra measured at point A (Figure 2) for the common (full line) and PWM (dotted line) mode

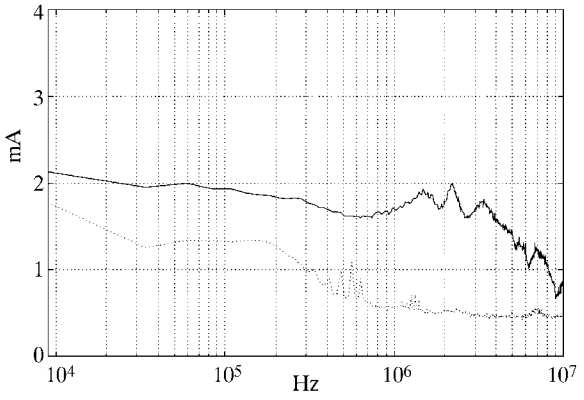

Fig. 15 Amplitude frequency spectra measured at point A (dotted line) and B (full line) for the differential mode (see Figure 3)

Figure 14 compares the amplitude frequency spectra measured at point A (Figure 2) for the common and PWM modes. The length of the cable $l_c = 10$ m. It can be seen that the complete noise spectrum for the applied PWM strategy is similar to that for the common mode.

Although the differential mode is also contained in the PWM mode, the PWM emission level is below that for the common mode. The reason is that the real waveforms of the PWM switch cycles have not a constant repeat frequency and the voltage change of U_d between the IM case and ground, occurring regularly in the common mode, is only occasional here; mostly only the change of $U_d/3$ is generated in the PWM mode.

Moreover, the contribution of the differential mode conducted emissions included in the total interference of the PWM mode is lower than that of the common mode (compare Figures 14 and 15). Figure 15 shows the amplitude frequency spectra for the differential mode measured at points A and B marked in Figure 3.

6. CONCLUSION

The theoretical background of the origins of the conducted as well as radiated emissions in the PWM inverter fed IM drives has been presented. The mechanisms of both common and differential current modes have been explained and a way of producing these modes independently by means of a suitable inverter control strategy introduced. The reason for that was the possibility to evaluate levels of the interference spectra of both the modes and compare contributions of different parts of the drive to the total emission level.

The main result is that the IM influences the emission level particularly up to 0.5–1 MHz, while the feeding cable is decisive for the waveforms of the amplitude frequency spectra.

The next step will be to select suitable methods for prediction of the conducted as well as radiated interferences based on measurable parameters of the system, providing basic information even in pre-production or application stages.

ACKNOWLEDGEMENT

The financial support of the Grant Agency of the Czech Republic (project No. 102/01/0182) is strongly acknowledged.

REFERENCES

[1] A. Orlandi, P. Tenti, A. Zuccato, A. Counsel, A. Testa, **Tutorial B: EMC in Power Electronics.** International Symposium on EMC'98, Roma, Italy, Sept. 1998.

[2] V. Valouch, J. Škramlík, I. Doležel, **Inverter-Fed Induction Motor Drive Model for Determining the Stray Current Disturbances.** Proc. of EMC'98, Roma, Italy, pp. 63–68, Sept. 1998.

[3] F. Klotz, J. Petzold, **Modelling of Conducted EMI.** Proc. of EPE'95, Sevilla, Spain, pp. 3356–3361, 1995.

[4] E. Hoene, W. John, H. Reichl, **Simulation of Conducted Electromagnetic Interference of Inverter-Fed Induction Motor.** Proc. of EPE'99, Lausanne, Switzerland, CD-ROM, 1999.

Visokofrekvencijski interferencijski signali generirani u sustavima s PWM izmjenjivačima, dugačkim kabelima i asinkronim motorima. Pri radu asinkronih izmjeničnih motora napajanih iz statičkih izmjenivača pojavljuju se visokofrekvencijski interferencijski signali koji su posljedica parazitnih struja između faza i parazitnih struja prema zajedničkoj točki. Ovi interferencijski signali mogu nepoželjno utjecati na rad obližnjih telekomunikacijskih i signalnih kabela i raznih elektroničkih uređaja. Ove se pojave u članku analiziraju teoretskim razmatranjima, koja su potkrijepljena eksperimentalnim rezultatima specijalnih mjerenja smetnji izazvanih parazitnim strujama. Evaluirane su uglavnom frekvencijske karakteristike odabranih dijelova sustava i njihov doprinos ukupnom harmonijskom spektru.

Ključne riječi: struje zajedničkog spoja, diferencijalne parazitne struje, visokofrekvencijski interferencijski signali, asinkroni motori, parazitne pojave

AUTHORS' ADDRESSES:

Prof. Ing. Viktor Valouch, CSc.
Ing. Jiří Škramlík
Prof. Ing. Ivo Doležel, CSc.
Institute of Electrical Engineering
Academy of Sciences of the Czech Republic
Dolejškova 5, 182 02 Praha 8
Czech Republic

Received: 2001–10–05